Pis'ma v ZhETF, vol. 91, iss. 2, pp. 89 – 96 © 2010 January 25

Dynamics and distribution of doped holes in the CuO_2 plane of slightly doped antiferromagnetic $YBa_2(Cu_{1-z}Li_z)_3O_{6+x}$ ($x < 0.1$) studied by Cu(1) NQR

A. V. Savinkov, A. V. Dooglav, H. Alloul, P. Mendels*, J. Bobroff*, G. Collin*, N. Blanchard**

Laboratory of Magnetic Resonance, Kazan State University, 420008 Kazan, Russia

**Laboratoire de Physique des Solides, Université Paris-Sud, UMR 8502, F-91405 Orsay, France*

Submitted 11 December 2009

Incidence of doped holes in the CuO_2 plane on the AF state was studied by Cu(1) nuclear quadrupole resonance (NQR) in slightly doped $YBa_2(Cu_{1-z}Li_z)_3O_{6+x}$ compounds. Inhomogeneous distribution of doped holes in the plane was detected in the low temperature measurements of transverse ($1/T_2$) and longitudinal ($1/T_1$) relaxation rates. We establish that at lower T the holes motion slows down and we estimate that the holes localize finally in restricted regions (~ 3 lattice constants) in the Coulomb potential of the Li^+ ions. Also we compared the hole behavior in slightly doped $YBa_2(Cu_{1-z}Li_z)_3O_{6+x}$ samples with that in slightly doped $Y_{1-y}Ca_yBa_2Cu_3O_6$. A stronger trapping potential of the in-plane Li^+ impurities was concluded as compared to slightly doped $Y_{1-y}Ca_yBa_2Cu_3O_6$ compound with out-of-plane Ca^{2+} impurities.

1. Introduction. Intensive studies for last two decades of the underdoped cuprates showed the occurrence at low temperatures of a magnetic-disordered state of the Cu^{2+} spin system in the CuO_2 plane with magnetic properties similar to that of the spin-glass systems [1 – 9].

A large amount of work has been devoted to the $La_{2-x}Sr_xCuO_4$ (LSCO) system, in which the "spin glass" behavior has been explained by the freezing of the spin degrees of freedom associated with the doped holes [2, 10]. The magnetic disordered state has been found quite different depending on hole doping.

(a) For hole contents $p_h < 0.02$ in LSCO such a low temperature magnetic disorder coexists with long-range antiferromagnetic (AF) order in the CuO_2 plane and with superconductivity at $0.05 < p_h < 0.1$. The doping dependence of the transition temperature into the magnetic-disordered state called "spin-glass" at the range $0 \le p_h \le 0.02$ was found to scale as $T_f \sim p_h$ [2, 3].

(b) For larger hole dopings only short-range AF exists in the CuO_2 plane, but the magnetic disordered state is observed up to $p_h \sim 0.1$ [5, 11, 12], i. e., the magnetic disorder coexists with superconductivity at $0.05 < < p_h < 0.1$. In this $0.02 \le p_h \le 0.1$ doping range the phase transition of the spin system in the CuO_2 plane into this low temperature "cluster spin-glass" state occurs at $T_g \sim 1/p_h$ [2, 12]. So, although most studies reveal inhomogeneous distributions of the doped holes, there is no consensus so far on the interpretation of their origin. Some suggest that at low doping the holes are self-organized in ensembles called "stripes", i. e., hole-rich "rivers" separated by antiferromagnetic boundaries (see, for example, Refs. [13 – 18]). Others, based mainly on experiments on other families of cuprates, consider the trapping potential of the dopant, defects, and disorder as sources of the inhomogeneity ! [10, 19 – 22].

Indeed, magnetic-disordered states of the CuO_2 spin system have also been found in other underdoped cuprates. The phase diagram [23] of underdoped $Y_{1-y}Ca_yBa_2Cu_3O_6$ ($YBCO_6$: Ca) in which the hole doping is controlled by the out-of-plane heterovalent substitution $Ca^{2+} \to Y^{3+}$ has been found to suggest [5] the existence of both the spin-glass and the cluster spin-glass states at $p_h < 0.035$ and $p_h > 0.035$, respectively. The slightly doped $YBCO_6$: Ca also reveal the inhomogeneous distribution of the doped holes at low temperatures. Authors of the EPR study [24] concluded that doped holes are organized in ordered structures in the CuO_2 plane, but our NQR studies evidence that the impurity ions play an important role for such hole inhomogeneity [25]. Also, the disorder due to ion substitution in the crystal structure was concluded as being the source for the cluster spin-glass state in underdoped $YBa_2Cu_3O_{6+x}$ ($0 < x < 0.5$) [22], i. e., for the hole inhomogeneity as well.

The phase diagram of LSCO in which the hole doping is controlled by the in-plane heterovalent substitution $Li^+ \to Cu^{2+}$ was found similar to that in LSCO and $YBCO_6$: Ca, a boundary between two types of low temperature magnetic disordered states was defined as $p_h \sim 0.03$ [26, 27]. However resistivity measurements do not show metallic behavior nor superconductivity in the $La_2Li_xCu_{1-x}O_4$ compound [28]. This fact suggests that behavior of the doped holes in the CuO_2 plane with

Li^+ impurities is different from that in the compound with out-of-plane impurity ions.

In this paper we report the results of an extensive study of the dynamics of doped holes and their distribution in the CuO_2 plane of the $YBa_2(Cu_{1-z}Li_z)_3O_{6+x}$ ($z = 0.005$, 0.01, 0.02, 0.04 and 0.06, $x < 0.1$) AF compound, in which the hole doping is achieved by the heterovalent substitution $Li^+ \to Cu(2)^{2+}$ in the CuO_2 plane. Such heterovalent substitution produces $3z/2$ holes per unit cell in the CuO_2 plane, i. e. the hole content in the samples must be $p_h \sim 0.0075$, 0.015, 0.03, 0.06 and 0.09, respectively. However as it was shown in [29], small batch-dependent part (15% maximum) of Li-atoms occupies the Cu(1) sites. Such substitution does not influence the hole doping of the planes. If we suggest homogeneous distribution of Li atoms in Cu(1) and Cu(2) sites then the hole doping is $p_h = z$. Thus estimation of the hole doping $p_h = 3z/2$ is the upper limit in our samples, but real doping is closer! to $p_h = 3z/2$ than to $p_h = z$, and hereafter we will suppose that all Li goes into the planes, so that $p_h = 3z/2$.

The Néel temperature exceeds 120 K for all samples. The conducting properties of slightly doped $YBa_2(Cu_{1-z}Li_z)_3O_6$ ($YBCO_6$: Li) are not known but this compound is not superconducting at any hole doping. This suggests that the behaviors of holes in $YBa_2Cu_3O_6$ with in-plane and out-of-plane impurities are rather different. To compare with the situation in the parent compound, we have done studies on the undoped sample $YBa_2Cu_3O_{6.09}$. Also we compared the hole behavior in slightly doped $YBCO_6$: Li samples with that in slightly doped $YBCO_6$: Ca [25].

2. Experimental procedure and results. The electronic magnetic moments of $Cu(2)^{2+}$ order antiferromagnetically below $T_N = 420$ K for pure $YBa_2Cu_3O_6$, both within the CuO_2 plane and between the adjacent planes, with moments aligned in the planes. A single bilayer of CuO_2 planes produces a hyperfine magnetic field of about 1 kOe on the Cu(1) nuclei [30]; but in the actual crystal it cancels out due to the symmetric position of Cu(1) with respect to the two neighboring Cu(2) ions pertaining to adjacent CuO_2 bilayers. So, for the nuclear spins of the nonmagnetic $Cu(1)^+$ ion one observes a pure nuclear quadrupole resonance (NQR) spectrum at $\nu_Q = 30.2$ MHz for ^{63}Cu at 4.2 K. A consequence of this cancellation of the internal field is that the Cu(1) nucleus is a good probe of what is happening in the planes. One can expect that the disturbance of the AF network by doped holes will inevitably break down this cancellation and influence both spectroscopic and dynamic properties of the Cu(1) nuclear spins. Such an influence was observed for $YBa_2Cu_3O_{6+x}$ ($x = 0.1$–0.4) [31] and for $YBCO_6$: Ca [25].

Samples of $YBCO_6$: Li, with $z = 0.005$, 0.01, 0.02, 0.04 and 0.06 and concentrations of oxygen $0.05 < x < 0.1$, and a reference powder sample of undoped $YBa_2Cu_3O_{6.09}$ were prepared by standard solid-state reaction. These samples are called below as Li0.5%, Li1%, Li2%, Li4%, Li6% and $YBCO_6$, respectively. A home-built-pulsed NMR/NQR spectrometer was used for measuring Cu(1) NQR spectra and relaxation.

2.1. *Transverse nuclear relaxation of Cu(1).* The transverse decay curves were obtained by varying the delay τ between the two radio frequency pulses of a standard spin-echo sequence $(\pi/2 - \tau - \pi)$ allowing to produce a spin echo $A(2\tau)$. For the transverse relaxation the fitting function used was

$$A(2\tau) = A(0)\exp\left[-(2\tau/T_2)^{N2}\right]. \qquad (1)$$

The spin-echo decay curves of Cu(1) nuclei in the reference $YBCO_6$ sample could be fitted well by Eq.(1) with $N2 \geq 1$, and was found independent of temperature in all the temperature range studied, from 4.2 to 300 K.

In all Li-samples a peak in the T variation of the transverse relaxation rate of Cu(1) is observed. At temperatures close to this peak temperature the spin echo decay curves cannot be fitted by Eq.(1), but at temperatures far from the peak a good fit is obtained with $N2 \sim 1$. One can perform a complete analysis of the data by assuming that there are two types of copper sites with different nuclear transverse relaxation rates. Similar behavior of the transverse relaxation Cu(1) was found in slightly doped $YBa_2Cu_3O_{6+x}$ ($0 \leq x \leq 0.4$) [31] and $Y_{1-y}Ca_yBa_2Cu_3O_6$ ($y = 0.02$ and 0.04) [25]. Then the best fitting procedure was obtained using Eq.(2) which includes a fraction P of fast relaxing component with a "stretched"-exponential relaxation curve and a long relaxing fraction $1 - P$ with a pure exponential relaxation curve (Fig.1),

$$A(2\tau) = A(0)\left\{P \cdot \exp\left[-\left(2\tau/T_{21}\right)^{N2}\right] + (1-P)\exp\left[-\left(2\tau/T_{22}\right)\right]\right\}. \qquad (2)$$

It was established for all Li-samples that the peak at low T corresponds to the fast relaxing Cu(1) nuclei (Fig.2a), and that the behavior of the slow relaxing Cu(1) nuclei is similar to that in undoped $YBCO_6$. Thus slow relaxing Cu(1) nuclei are not "sensitive" to hole doping. The N2 parameter in function (2) related to the fast relaxing Cu(1) reaches a minimum value at the temperatures of the peak (Fig.2b).

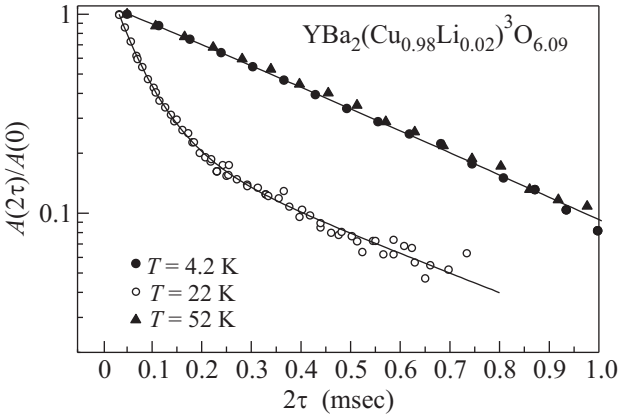

Fig.1. The Cu(1) echo decay curves in the Li2% sample at certain temperatures. Solid lines are fitting results by Eq.(2), which resumes to the single component Eq.(1) for the two extreme temperatures, 52 and 4.2 K

In all $YBCO_6$: Li samples we detected another peak in the transverse relaxation rate Cu(1) at $T \sim 65-70$ K. The temperature of the peak doesn't depend on the hole content and the maximum value of $1/T_2$ increases with doping. A similar behavior of the Cu(1) nuclear transverse relaxation at $T \sim 65-70$ K was observed in slightly doped $YBa_2Cu_3O_{6+x}$ ($0.1 \leq x \leq 0.4$) [31] and $Y_{1-y}Ca_yBa_2Cu_3O_6$ ($y = 0.02$ and 0.04) [25]. In this temperature range the analysis of the spin-echo decay curves measured in the $YBa_2(Cu_{1-z}Li_z)_3O_6$ ($z = 0.02$, 0.04 and 0.06) samples showed that it is not possible to separate the curves into two contributions by Eq.(2). Good fits are obtained with Eq.(1) with a nearly exponential behavior (that is $N2 \sim 1$) (Fig.2b). Thus we conclude that the peak at $T \sim 65-70$ K in samples with $z = 0.02$, 0.04 and 0.06 is due to transverse relaxation rate enhancement of all Cu(1) nuclei. In samples with the smallest Li substitutions ($z = 0.005$ and 0.01) fitting by Eq.(1) gives $N2 < 1$ at $T \sim 65-70$ K. This evidences a distribution of the transverse relaxation rates, i. e. only part of Cu(1) nuclei shows an enhanced transverse relaxation.

2.2. *Longitudinal nuclear relaxation of Cu(1).* The longitudinal relaxation recovery curves were obtained using the standard three-pulse techniques $(\pi/2) - t' - (\pi/2 - \tau - \pi)$ where the first $\pi/2$ pulse saturates the NQR line, and the spin-echo sequence allows to measure the recovery $A(t')$ of the longitudinal nuclear magnetization after the evolution time t'. The curves measured for all samples were fitted by function:

$$A(t') = A(\infty)\left\{1 - B \cdot \exp\left[-(t'/T_1)^{N1}\right]\right\}. \quad (3)$$

Data for the undoped reference sample are well fitted in all the (4.2 – 150 K) temperature range with $N1 \sim 0.65$, i. e. suggesting non-exponential relaxation; the $1/T_1$ was found almost temperature independent. The data analysis using function (3) showed a peak in the T dependencies of $1/T_1$ in the Li-samples with $z = 0.02$, 0.04 and 0.06 at $T \sim 50$ K, ~ 31 K and ~ 29 K, respectively (Fig.3a). Such a peak in the longitudinal relaxation of Cu(1) was not found in the Li-samples with $z = 0.005$ and $z = 0.01$.

For the Li-samples with $z = 0.04$ and 0.06, the longitudinal relaxation recovery curves measured at temperatures close to the $1/T_1$ peak values cannot be fitted well enough by function (3). As for the T_2 analysis, the shape of the curves suggests two contributions in the longitudinal relaxation originating from two kinds of Cu(1) nuclei

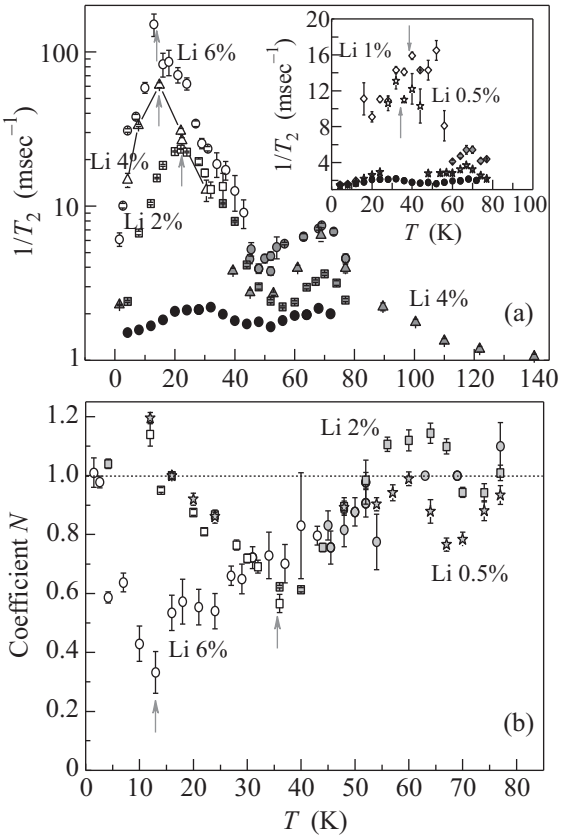

Fig.2. (a) Temperature dependence of transverse nuclear relaxation rate of ^{63}Cu(1) in the samples Li6% (circles), Li4% (triangles), Li2% (squares) and $YBCO_6$ (black circles). Gray symbols represent the $T_2{}^{-1}(T)$ obtained from experimental data with fitting function (1), open symbols are $T_{21}{}^{-1}(T)$ of the fast relaxing Cu(1) nuclei obtained with fitting function (2) for $YBCO_6$: Li. Inset: T-dependence of the $T_2{}^{-1}(T)$ of ^{63}Cu(1) in the samples Li1% (rhomboids), Li0.5% (stars) and $YBCO_6$ (black circles). Gray arrows point to the $T_{21}{}^{-1}(T)$ peaks. (b) T-dependence of N2 in Equation (2) for the samples Li6% (circles), Li2% (squares) and Li0.5% (stars). Gray arrows point to the minimum of N2

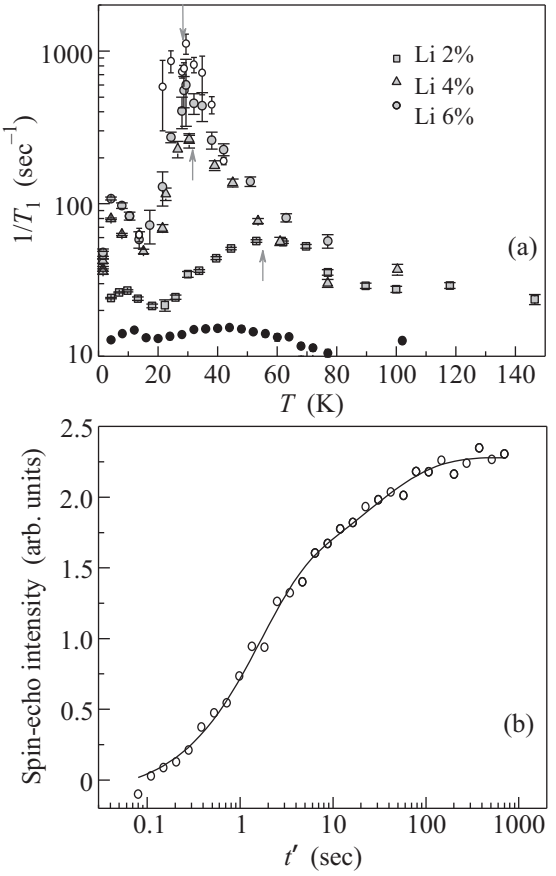

Fig.3. (a) The temperature dependence of the longitudinal relaxation rate of ^{63}Cu(1) in the samples Li6% (grey circles), Li4% (grey triangles), Li2% (grey squares) and reference sample $YBCO_6$ (black circles). The values of $1/T_1$ are obtained by fitting the longitudinal relaxation recovery curves by function (3). The $1/T_{11}$ of fast relaxing Cu(1)'s for the Li6% sample (open circles) were obtained by Eq.(4) as discussed in the text. Gray arrows point to the $1/T_{11}$ peaks. (b) Longitudinal relaxation recovery curve for the Li6% sample measured at temperature $T = 28.7$ K (open circles). The solid line is the best fit by Eq.(4)

with very different relaxation rates (Fig.3b). This distinction by $1/T_1$ of two kinds of Cu(1) nuclei was also found in slightly doped $Y_{1-y}Ca_yBa_2Cu_3O_6$ ($y = 0.02$ and 0.04) [25]. There it was found that the longitudinal relaxation was enhanced only for part of the Cu(1) nuclei. Other Cu(1) nuclei keep a T_1 value equal to that out of the peak in ${T_1}^{-1}(T)$, close to that of the undoped reference sample. The longitudinal relaxation recovery curves were fitted by function [25]:

$$A(t') = A(\infty)\cdot\left[\left\{1 - B\cdot\exp\left[-(t'/T_{11})^{N11}\right]\right\} + \right.$$
$$\left. + C\cdot\left\{1 - B\cdot\exp\left[-(t'/T_{12})^{N12}\right]\right\}\right], \qquad (4)$$

where T_{11} and T_{12} were the longitudinal relaxation times of fast and slow relaxing Cu(1) nuclei. We applied this function to our data measured for the Li6% sample (an example of fit for $T = 29$ K is shown in Fig.3b). The values of $1/T_{12}$, N_{12} and the saturation factor B obtained at certain temperatures out of the $1/T_1$ peak were imposed in the fits of the function (4). The $1/T_{11}(T)$ values for fast relaxing Cu(1) nuclei are shown in Fig.3a. For the Li2% and Li4% samples the difference between relaxation rates of fast and slow relaxing Cu(1) were found rather small as compared to that found for $YBCO_6$: Ca samples. Therefore the fits with Eq.(4) do not give reliable estimates of the relaxation parameters for these z values. Nevertheless we can conclude that in slightly doped $YBa_2(Cu_{1-z}Li_z)_3O_6$ with $z > 0.02$ the Cu(1) nuclei also separate into fast and slow relaxing components.

3. Discussion. 3.1. *Low temperature "spin-glass" state.* The ^{139}La NQR data obtained in the undoped La_2CuO_4 compound with spin-less Zn^{2+} impurities which substitute the plane Cu^{2+} ions has revealed that a peak in the T dependence of $1/T_1$ occurs at temperatures of about 70 – 100 K [32]. The authors suggest that this modification of the longitudinal relaxation rate can be driven by fluctuations of local moments induced by spin-less impurities. In reference [25], an undoped $YBCO_6$: Zn,Tm compound was studied, where a small part (2%) of the $Cu(2)^{2+}$ plane ions was substituted by the iso-valent Zn^{2+} spin-less impurity and 5% of Y^{3+} were substituted by iso-valent Tm^{3+}. Due to the different ionic radii, such substitutions still create some disorder in the YBCO structure. However, no modification of the longitudinal and transverse relaxation rates of Cu(1) nuclei was found at low temperatures.

Therefore the peaks in the Cu(1) relaxation rates observed in $YBCO_6$: Li are not driven by the disorder introduced by impurities. We rather conclude that it is the slowing down of the doped holes motion that gives rise to slow magnetic fluctuations on the Cu(1) sites and results in the enhancement of the longitudinal and transverse relaxations of Cu(1) nuclei at low temperatures. This is supported by the fact that a similar behavior of the Cu(1) relaxation is observed in other lightly doped YBCO cuprates: $YBa_2Cu_3O_{6+x}$ ($0.1 \le x \le 0.4$) [31] and $Y_{1-y}Ca_yBa_2Cu_3O_6$ ($y = 0.02$ and 0.04) [25]. Unfortunately the accuracy of our $1/T_1$ and $1/T_2$ data for fast relaxing copper were not enough to decide whether the relaxations are produced by fluctuating magnetic or electric field. In $YBCO_6$: Ca the $1/T_2$ of fast relaxing ^{65}Cu(1) at the peak temperature was larger than that for ^{63}Cu(1). Since the gyromagnetic ratio for ^{65}Cu is larger than for ^{63}Cu, contrary to the quadrupole moments, this indicates the magnetic origin of the relaxation. We can

also conclude that the transverse relaxation in our case is not determined by the nuclear magnetic dipole-dipole interactions, because the natural abundance of ^{65}Cu is more than two times less than that of ^{63}Cu, and $1/T_2$ for ^{65}Cu would be less than for ^{63}Cu due to this mechanism.

The peak in longitudinal relaxation rate appears when the fluctuations become slow enough to reach the Cu(1) NQR frequency $3{\cdot}10^7$ Hz. As for the enhancement of the transverse relaxation rate, it only occurs when the rate of magnetic fluctuations becomes as low as $1/T_2$, i. e., of the order of tens kHz [33, 34]. The enhancement of the nuclear longitudinal relaxation rate is produced by the fluctuations of magnetic field perpendicular to the quantization axis of the nuclear-spin system [35]. On the contrary, the enhancement of transverse relaxation rate is produced mainly by the low-frequency fluctuations parallel to the quantization axis [35].

In $YBCO_6$: Li in the absence of external magnetic field, the quantization axis for the nuclear spins of the twofold-coordinated Cu(1) coincides with the principal axis of the axially symmetric tensor of electric-field gradient and is parallel to the crystallographic c axis. The existence of peaks for both longitudinal and transverse relaxation rates indicates that the fluctuating magnetic fields have components both perpendicular and parallel to the c-axis. The latter apparently appear due to the out-of-plane components of the electronic magnetic moments of $Cu(2)^{2+}$ located near the doped hole [2, 3, 10]. The enhancement of the longitudinal relaxation rate, which can be assigned to the loss of hyperfine field compensation at the Cu(1) site was observed in our $YBCO_6$: Li only for dopings $p_h \geq 0.03$ ($z \geq 0.02$). But the $1/T_2$ peak caused by the fluctuating out-of-plane component of the $Cu(2)^{2+}$ is observed in all Li-doped samples, i. e. at $p_h \geq 0.0075$. Both kinds of magnetic fluctuations occur due to the motion of the doped holes in the CuO_2 plane. In Ref. [36] authors showed that heterovalent substitution in cuprates (of the kind $Ca^{2+} \to Y^{3+}$ in $YBCO_6$: Ca) gives rise to the appearance of the thermally activated doped holes in the CuO_2 plane.

The freezing of these spin degrees of freedom in the slightly doped $La_{2-x}Sr_xCuO_4$ ($x < 0.02$) [2, 5], $La_2Cu_{1-z}Li_zO_4$ ($z < 0.03$) [27], and $Y_{1-y}Ca_yBa_2Cu_3O_6$ ($y < 0.07$) [5] at $T < T_f$ gives rise to the transition of the plane Cu^{2+} spin system into the disordered magnetic state called "spin glass" which is superimposed on the pre-existing AF long-range order with $T_f \sim p_h$. The T_f obtained in our study as the peak temperature in $T_2^{-1}(T)$ is smaller in Li0.5% ($p_h = 0.0075$) than in Li1% ($p_h = 0.015$): respectively, 32 K and 38 K (Fig.4). These data suggest that the

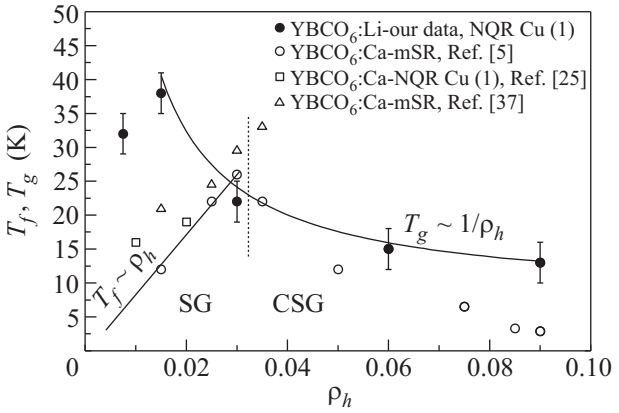

Fig.4. T_f and T_g in slightly doped $YBCO_6$: Li and $YBCO_6$: Ca. SG and CSG are spin-glass and cluster spin-glass states in the picture

Cu(2) spin system in $YBCO_6$: Li ($z \leq 0.01$) transfers at $T < T_f$ to the type of low temperature spin-glass state reported in Ref. [2, 5, 27]. The linear behavior of T_f has been explained theoretically in [10] if the freezing of transverse degrees of freedom is associated with the many-Skyrmion spin texture produced by randomly distributed defects. Our samples do not show the linear behavior of T_f as well as that found in $YBCO_6$: Ca [25, 37] and LSCO [15].

In the $YBCO_6$: Li with $z \geq 0.02$ ($p_h \geq 0.03$) the transition temperature to the disordered magnetic state obtained as the peak temperature in the Cu(1) transverse relaxation rate becomes lower with increasing hole doping (Fig.4). Such an evolution is consistent with the transition below T_g of the plane Cu^{2+} spin system into the disordered magnetic state called "cluster spin glass" with $T_g \sim 1/p_h$ [1, 5, 27]. In reference [20] the interactions between more than two Skyrmion impurity states was considered as a possible origin of the cluster spin glass phase. The CuO_2 spin system undergoes a phase transition into the cluster spin glass state at $T < T_g$ in which the clusters of the AF correlated spins freeze due to their mutual interaction below T_g estimated by authors of Ref. [2] as $T_g \sim 1/p_h$. In YBCO6: Li with $z \geq 0.02$ ($p_h \geq 0.03$) the temperatures of the $1/T_2$ peaks, which might be assimilated to T_g, ! has an evolution with hole doping close to $T_g \sim 1/p_h$. Thus the boundary in the phase diagram between two kinds of the disordered magnetic states is located in the range $0.015 \leq \leq p_h \leq 0.03$. This boundary in the $La_2Cu_{1-z}Li_zO_4$ was found at $z = p_h \sim 0.03$ [27].

3.2. *Doped hole distribution in the CuO_2 plane.* The origin of the peaks in the Cu(1) transverse relaxation rate at $T \sim 65-70$ K is not clear now. This peak was found in slightly doped $YBa_2Cu_3O_{6+x}$ [31]

Fraction P of the fast relaxing Cu(1) nuclei and area S of the CuO_2 plane occupied by localized holes at the T of the $1/T_2$ peak in the samples $YBCO_6$: Li and $YBCO_6$: Ca [25]

Sample	$YBa_2(Cu_{1-z}Li_z)_3O_6$					$Y_{1-y}Ca_yBa_2Cu_3O_6$	
x, z	0.005	0.01	0.02	0.04	0.06	0.02	0.04
(p_h)	(0.0075)	(0.015)	(0.03)	(0.06)	(0.09)	(0.01)	(0.02)
P	27(3)%	57(2)%	89(2)%	86(2)%	89(2)%	60(4)%	85(3)%
S	14(2)%	34(2)%	67(2)%	63(2)%	67(2)%	~40%	~60%

and $Y_{1-y}Ca_yBa_2Cu_3O_6$ ($y = 0.02$ and 0.04) [25] compounds, but was not found in our undoped $YBCO_6$ nor in undoped $YBCO_6$: Zn,Tm [25]. Thus we assume that the $1/T_2$ peak at $T \sim 65-70$ K is due to mobile holes behavior and not due to the disorder. In [25] we concluded that the homogeneous distribution and free motion of the doped holes occurred above the temperature of this peak in slightly doped $YBCO_6$: Ca. Even at the doping $p_h = 0.01$ an enhancement of the transverse relaxation rate was seen for all Cu(1) nuclei. As for Li samples studied here, fitting the $T \sim 65-70$ K data by equation (1) shows an enhancement of all Cu(1)'s in our $YBCO_6$: Li samples only for $z > 0.02$ ($p_h > 0.03$). Thus the holes in slightly doped $YBCO_6$: Li compound with in-plane Li^+ impurities seem to be more bound with the impurity center than in slightly doped $YBCO_6$: Ca compound with out-of-plane Ca^{2+}.

The observed separation of the transverse and longitudinal relaxation rates of Cu(1) nuclei into two kinds evidences an inhomogeneous distribution of the doped holes at low temperatures. The impurity ions likely play an important role in this inhomogeneous distribution of the holes and in the emergence of spin-glass behavior, as it takes place, for example, in LSCO, where part of trivalent La^{3+} is replaced by divalent Sr^{2+} [10, 20]. It is natural then to assume that the in-plane Li^+ ions, which are centers of electrostatic attraction for the holes as well, are the relevant pinning centers for the doped holes. Therefore at low temperatures one can expect that the motion of the doped holes is localized in the vicinity of the Li^+ sites, so that the fraction P of fast relaxing Cu(1) nuclei (see Table), which sense the slow magnetic fluctuations induced by slow motion of the doped holes in the CuO_2 plane, is a measure of the spatial extent of the regions with localized holes. The fraction $1-P$ of other Cu(1) nuclei has relaxation rates similar to that at Cu(1) in hole-free $YBCO_6$ which points out that they are far enough from the regions where holes localize.

The area occupied by holes at the temperatures of the peak in $1/T_2$ Cu(1) can be estimated from the fraction P of fast relaxing Cu(1). In this case the area is defined as $S = 1-\sqrt{1-P}$ if the hole motion is not correlated in adjacent CuO_2 planes. The obtained values of the area S are gieven in Table for all $YBCO_6$: Li samples. However if one of the components in the Cu(1) transverse relaxation rate exceeds the other one by more than a factor 4 or 5, the error on the estimated P becomes substantially bigger than that shown in Table. Moreover S has a fast variation for P values close to 1. For example, a variation of P from 0.9 to 1.0 changes S from 0.68 to 1. Thus the estimation of the area occupied by doped holes seems not very reliable for $YBCO_6$: Li samples with $z > 0.02$. However, comparing the area S in slightly doped samples $YBCO_6$: Ca [25] and $YBCO_6$: Li at similar hole doping suggests stronger bonding of the holes with n-plane Li^+ ions than with out-of-plane Ca^{2+} ions.

Our present study also allowed us to evidence that the freezing of the magnetic fluctuations at Cu(1) site occurs in $YBCO_6$: Li at higher temperatures than in $YBCO_6$: Ca (Fig.4). This also suggests a stronger trapping potential of the in-plane Li^+ impurities. The stronger influence of the Li^+ impurity potential on the doped holes is also supported by the other facts. First, the superconductivity in $YBCO_6$: Li is not induced at any doping level, while $YBCO_6$: Ca shows superconducting properties at high enough doping [38]. Second, Cu(2) ZFNMR experiments performed in $YBCO_6$: Ca and $YBCO_6$: Li [39] showed wipe-out effect in the $YBCO_6$: Ca compound, but in $YBCO_6$: Li the wipe-out effect wasn't complete for similar hole dopings. Moreover, muon spin rotation experiments in the same compounds showed that T_N decreases slower with doping in $YBCO_6$: Li than in Ca-doped $YBCO_6$ (Fig.5).

The size of the microscopic regions occupied by holes cannot be directly obtained from our NQR experimental data and requires at least some further analysis. In [25] we estimated the size of the regions by using a simple model in which the doped holes regions formed around Ca^{2+} impurities are disks in the CuO_2 plane. Square samples (100×100 lattice constants) of the CuO_2 plane were considered, with the Ca impurities at random positions. The disk diameter was increased until the total fractional area occupied by the disks reached for both samples of $YBCO_6$: Ca the experimental values of S obtained from NQR data. This procedure took into account the overlapping of the disks. Radius of the disks

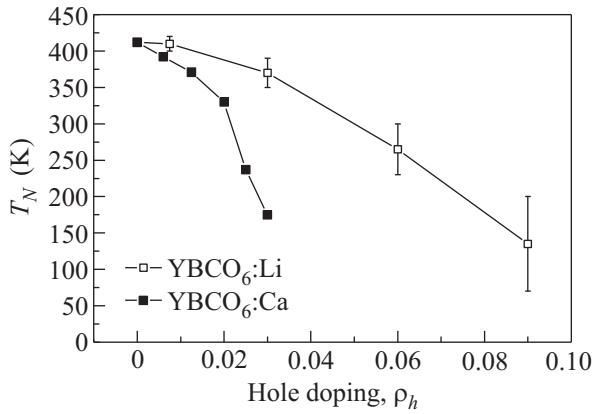

Fig.5. Comparison between the Néel temperature for $YBCO_6$: Ca with that for $YBCO_6$: Li compounds obtained from muon spin rotation

for $YBCO_6$: Ca ($p_h \sim 0.01$ and 0.02) samples was estimated as $r_h \sim 4$ lattice constants at temperature of the peaks in $1/T_2$. Using the same model for our $YBCO_6$: Li samples with $p_h \sim 0.0075$, 0.015 and 0.03 we obtained $r_h \sim 3$ lattice constants. Even taking into account that the real hole doping p_h in our samples might be slightly less than $3z/2$, the estimation of r_h will not change drastically. The distance between impurities in the CuO_2 planes is $l \approx 1/\sqrt{p_h}$, so the size S of the disks for samples with $z \leq 0.02$ is less than the mean distance, i. e. $2r_h \leq l$. Thus one can explain the linearity of $S(p_h)$ with hole doping at $z \leq 0.02$ obtained from the Table data by assuming that the single impurity regime occurs then in the CuO_2 plane. In this regime the microscopic regions occupied by doped holes are not overlapping. One expects that at temperatures much smaller than T_f, the doped holes are completely localized on fixed orbitals around the Li^+.

4. Conclusion. In conclusion, our Cu(1) NQR study of slightly doped $YBa_2(Cu_{1-z}Li_z)_3O_{6+x}$ has provided evidence for an inhomogeneous distribution at low temperatures of the holes doped into the CuO_2 plane by the heterovalent substitution $Li^+ \rightarrow Cu(2)^{2+}$. It was found that part of the Cu(1) nuclei has the same transverse relaxation rate as in undoped $YBa_2Cu_3O_{6.09}$ sample. Thus part of the Cu(1) nuclei does not sense any hole motion in the CuO_2 plane. This inhomogeneous distribution of doped holes was also detected in the low T measurements of $1/T_1$, in the samples with $z \geq 0.02$. At low temperatures the doped holes localize in restricted regions in the vicinity of the Li^+ pinning centers. The analysis of the spin-echo decay curves has allowed us to show that the area of these regions in the CuO_2 plane scales with p_h at the smallest hole dopings. At the temperature at which $1/T_2$ is maximal, the radius of the regions occupied by holes is estimated as $r_h \sim 3$ lattice constants around the impurity ions. This value is less than that estimated for $YBCO_6$: Ca samples [25]. Moreover, the distribution of the Cu(1) nuclear relaxation rates observed at the second peak value of $1/T_2$ ($T \sim 65-70$ K) also suggests that doped holes are more strongly bound with the in-pane Li^+ ion than with the out-of-plane Ca^{2+} ions in $Y_{1-y}Ca_yBa_2Cu_3O_6$.

The observed peaks in $1/T_2$ and $1/T_1$ allowed us to evidence that a slowing down of the magnetic fluctuations at the Cu(1) sites is induced by the doped hole motion. The evolution with doping of the transition temperature to the magnetic disordered state suggests that the low temperature "spin-glass" regime occurs in the $YBCO_6$: Li samples at small hole doping $p_h < 0.015 - 0.03$ and that the "cluster spin-glass" regime occurs for larger Li dopings. The boundary between these two regimes is close to that ($p_h \sim 0.03$) found for $La_2Li_xCu_{1-x}O_4$ compounds [26, 27].

1. J. H. Cho, F. Borsa, D. C. Johnston et al., Phys. Rev. B **46**, 3179 (1992).
2. F. C. Chou, F. Borsa, J. H. Cho et al., Phys. Rev. Lett. **71**, 2323 (1993).
3. F. Borsa, P. Carretta, J. H. Cho et al., Phys. Rev. B **52**, 7334 (1995).
4. D. R. Harshmann, G. Aeppli, G. P. Espinosa et al., Phys. Rev. B **38**, 852 (1988).
5. Ch. Niedermayer, C. Bernhard, T. Blasius et al., Phys. Rev. Lett. **80**, 3843 (1998).
6. B. Keimer, N. Belk, R. J. Birgeneau et al., Phys. Rev. B **46**, 14034 (1992).
7. S. Wakimoto, R. J. Birgeneau, M. A. Kastner et al., Phys. Rev. B **61**, 3699 (2000).
8. F. C. Chou, N. R. Belk, M. A. Kastner et al., Phys. Rev. Lett. **75**, 2204 (1995).
9. M. E. Filipowski, J. I. Budnick, and Z. Tan, Physica (Amsterdam) C **167**, 35 (1990).
10. R. J. Gooding, N. M. Salem, and A. Mailhot, Phys. Rev. B **49**, 6067 (1994).
11. C. Panagopoulos, B. D. Rainford, J. R. Cooper et al., Physica C **341**, 843 (2000).
12. M.-H. Julien, Physica B **329**, 693 (2003).
13. V. J. Emery, S. A. Kivelson, and J. M. Tranquada, Proc. Natl. Acad. Sci. U.S.A. **96**, 8814 (1999).
14. J. M. Tranquada, B. J. Sternlieb, J. D. Axe et al., Nature (London) **375**, 561 (1995).
15. M. Matsuda, M. Fujita, K. Yamada et al., Phys. Rev. B **65**, 134515 (2002).
16. L. P. Pryadko, S. A. Kivelson, and D. W. Hone, Phys. Rev. Lett. **80**, 5651 (1998).
17. A. Paolone, F. Cordero, R. Cantelli et al., Phys. Rev. B **66**, 094503 (2002).

18. M. Bosch and Z. Nussinov, arXiv:cond-mat/0208383.
19. A. Aharony, R. J. Birgeneau, A. Coniglio et al., Phys. Rev. Lett. **60**, 1330 (1988).
20. R. J. Gooding, N. M. Salem, R. J. Birgeneau et al., Phys. Rev. B **55**, 6360 (1997).
21. H. Alloul, J. Bobroff, M. Gabay et al., Rev. Modern Physics **81**, 45 (2009).
22. S. Sanna, G. Allodi, G. Concas et al., J. Supercond. **18**, 169 (2006).
23. H. Casalta, H. Alloul, and J.-F. Marucco, Physica C **204**, 331 (1993).
24. A. Janossy, T. Feher, and A. Erb, Phys. Rev. Lett. **91**, 177001 (2003).
25. A. V. Savinkov, A. V. Dooglav, H. Alloul et al., Phys. Rev. B **79**, 014513 (2009).
26. B. J. Suh, P. C. Hammel, Y. Yoshinary et al., Phys. Rev. Lett. **81**, 2791 (1998).
27. T. Sasagawa, P. K. Mang, O. P. Vajk et al., Phys. Rev. B **66**, 184512 (2002).
28. M. A. Kastner, R. J. Birgeneau, C. Y. Chen et al., Phys. Rev. B **37**, 111 (1998).
29. J. Bobroff, W. A. MacFarlane, H. Alloul et al., Phys. Rev. Lett. **83**, 4381 (1999).
30. A. V. Dooglav, H. Alloul, M. V. Eremin et al., Physica C **272**, 242 (1996).
31. M. Matsumura, H. Yamagata, and Y. Yamada J. Phys. Soc. Jpn. **58**, 805 (1989).
32. M. Corti, A. Rigamonti, F. Tabak et al., Phys. Rev. B **52**, 4226 (1995).
33. S. Fujiyama, M. Takigawa, and S. Horii, Phys. Rev. Lett. **90**, 147004 (2003).
34. M. Takigawa and G. Saito, J. Phys. Soc. Jpn. **55**, 1233 (1986).
35. C. P. Slichter, *Principles of Magnetic Resonance*, Springer-Verlag, New York, 1990.
36. S. Sanna, F. Coneri, A. Rigoldi et al., Phys. Rev. B **77**, 224511 (2008).
37. C. E. Stronach, D. K. Noakes, X. Wan et al., Physica C **311**, 19 (1999).
38. J. L. Tallon, C. Bernhard, H. Shaked et al., Phys. Rev. B **51**, 12911 (1995).
39. P. Mendels, private communication.